

CORRECTING STRUCTURED ILLUMINATION ABERRATION EFFECTS IN STRUCTURED  
ILLUMINATION MICROSCOPY

by

Alex Jacobson

---

Copyright © Alex Jacobson 2022

A Thesis Submitted to the Faculty of the

JAMES C. WYANT COLLEGE OF OPTICAL SCIENCES

In Partial Fulfillment of the Requirements

For the Degree of

MASTER OF SCIENCE

In the Graduate College

THE UNIVERSITY OF ARIZONA

2022

THE UNIVERSITY OF ARIZONA  
GRADUATE COLLEGE

As members of the Master's Committee, we certify that we have read the thesis  
prepared by: Alex Jacobson

titled: CORRECTING STRUCTURED ILLUMINATION ABERRATION EFFECTS IN STRUCTURED  
ILLUMINATION MICROSCOPY

and recommend that it be accepted as fulfilling the thesis requirement for the Master's Degree.

*Leilei Peng*

\_\_\_\_\_  
Leilei Peng

Date: May 3 2022

*Rongguang Liang*

\_\_\_\_\_  
Rongguang Liang

Date: May 3 2022

*[Signature]*

\_\_\_\_\_  
Khanh Kieu

Date: May 3 2022

Final approval and acceptance of this thesis is contingent upon the candidate's submission of the  
final copies of the thesis to the Graduate College.

I hereby certify that I have read this thesis prepared under my direction and recommend that it be  
accepted as fulfilling the Master's requirement.

*Leilei Peng*

\_\_\_\_\_  
Leilei Peng

Thesis Committee Chair  
College of Optical Sciences

Date: May 3 2022

## Table of Contents

List of Figures .....	4
Abstract .....	5
Chapter 1: Methods for Enhancing Spatial Resolution.....	6
Chapter 2: The Theory of Structured Illumination Microscopy .....	10
Chapter 3: Aberration Correction Theory and Simulation.....	13
Chapter 4: Conclusions and Future Work .....	25
Appendix.....	26
References .....	33

## List of Figures

Figure 1: Conceptual 1D Linear SIM Patches .....	12
Figure 2: Simulated Target and Sum of Raw Data.....	15
Figure 3: 1D Superresolution SIM with no Aberration Effects in Structured Illumination	16
Figure 4: 1D Superresolution SIM with 1 Wave Aberration Effects .....	17
Figure 5: 1 Wave Phase Map .....	18
Figure 6: Distorted 1D Structured Illumination.....	19
Figure 7: Comparison of Lightsheet and Superresolution Structured Illumination.....	20
Figure 8: Recovered Phase Map .....	21
Figure 9: Unwrapped Recovered Phase Map.....	22
Figure 10: Simulated 1D Superresolution SIM.....	23
Figure 11: Simulated Random Fiber Target SIM.....	24

## **Abstract**

The resolution of an optical microscope is limited to roughly 250 nm for biological imaging. This is due to the wave nature of light which causes an optical system to be diffraction limited according to the wavelength of light involved and the numerical aperture of the system. In order to image finer structural details of biological samples it is necessary to image beyond the diffraction limit. There are several methods for doing this. One method for imaging beyond the diffraction limit is structured illumination microscopy (SIM), a type of fluorescence microscopy where high frequency information is put into low frequency space by using a periodic illumination pattern at different phases. One of the difficulties with this method is that experimentally the periodic illumination pattern will never be ideal since it will suffer from the aberration effects of the system. This thesis presents a computer program with an algorithm to correct for the aberration effects in the periodic illumination which corrects independent of any specific type of aberration introduced into the structured illumination. The computer program first simulates one dimensional linear SIM, adds in aberration effects, and then corrects the image. The results show that the algorithm improves the superresolution image for the conditions of 0.5 wave, 1 wave, and 2 wave aberration effects in the structured illumination. With this computer program as a foundation, future work could expand the program to include two-dimensional nonlinear SIM for experimental applications.

## Chapter 1: Methods for Enhancing Spatial Resolution

An optical imaging system uses electromagnetic waves to represent an object in the form of an image. The waves can transmit, reflect or be absorbed by the object. In the case of fluorescence microscopy, fluorophores absorb light at a short wavelength and emit light at a longer wavelength. The imaging system operates on the object to produce the image as

$$g = Hf + n \quad (1)$$

where  $H$  is the imaging system operator and  $g$ ,  $f$ , and  $n$  are functions of the image, object and noise respectively. Fluorescence microscopy uses emission from discrete objects – fluorophores. Since the fluorophores are the object, we are one step removed from imaging the sample which holds implications for structural information. To know how well the image represents the object quantitatively would help with measuring the trustworthiness of the information obtained from the image. When the object is fully known we can compare the object and the image using cross correlation but when the object is unknown or partially known we must use a metric based on the type of information that we want to obtain about the object. The latter case is known as an objective task-based assessment of image quality. Resolution, in the broadest sense, is the ability to distinguish between two different points in space or time. The choice of method for measuring the resolution in the image depends on the task at hand. Spatial resolution can be used as the task for image quality in fluorescence microscopy. Depending on the given task resolution may or may not be a limiting factor. Other limiting factors could include Signal to Noise Ratio (SNR), Field of View (FOV), magnification, and wavelength. In early optical microscopy, spatial resolution was practically limited by aberrations and was greatly improved throughout the centuries to the point that the effect of diffraction became a limiting factor in lens design in the late 1800's. Later, Abbe, Helmholtz, and Rayleigh determined the limit that diffraction puts on spatial resolution starting with Abbe in 1873. Diffraction limits the far field spatial resolution to

$$R \propto \frac{\lambda}{NA} \quad (2)$$

with proportionality constants depending on the aperture and how resolution is defined. The optical transfer function (OTF) describes the range of spatial frequencies that the image contains. The effect of diffraction is to spread out the spatial frequencies so that the high frequencies are cutoff as the light goes through the pupil function of the lens. This means a lens acts as a low pass filter so that the OTF goes to zero at high frequencies. Enhancing the resolution refers to expanding the total range over which the OTF exists and not merely reshaping the OTF. A type of microscope known as superresolving microscopes were invented in 1963 with a microscope that improved the spatial resolution by decreasing the temporal resolution [1]. A 1966 paper describes other superresolving methods including increasing the OTF by decreasing the FOV, extending the OTF in one spatial dimension by decreasing it in another and increasing the OTF in one polarization by decreasing it in another [2]. All these methods increase the OTF in one degree of freedom while reducing it in another to keep the number of degrees of freedom constant [2]. After these methods a microscope that used the near field to improve the resolution was developed. Near field scanning optical microscopy (NSOM) uses diffraction to transform evanescent waves into propagating waves [3]. NSOM is limited to imaging topologically and suffers from convolution of the object with the probe making it unsuitable for structures with depth. Starting with the STED microscope in 1994 a new category of far field microscopes was formed where the OTF was expanded without reducing the bandwidth in any of the degrees of freedom [4]. This new category includes point scanning, stochastic pointillism and wide field methods and is called superresolution microscopy. Superresolution microscopy in this context means that the spatial resolution is theoretically unlimited. One method of superresolution is to use Reversible Saturable Optical Fluorescence Transitions (RESOLFT). In this point scanning method, the fluorophores are driven to one of two states depending on their location. One beam puts the

fluorophores of a given PSF into a state A and the second beam with the same PSF except for a near zero point at the center puts the fluorophores in a state B. Forming the shape of the second beam and the timing between the arrival of these two beams are two important design considerations for RESOLFT. In the case where the second beam uses stimulated emission depletion (STED), the shape is formed by a helical phase plate which creates a first order optical vortex. The phase plate consists of one full revolution of steps with the height between the tallest step and the lowest on the order of magnitude of the design wavelength. The STED beam uses powers near the gigawatt range which accelerates fluorophore photo bleaching, may damage the sample and make this method not ideal for biological studies. PALM (Photoactivable Localization Microscopy) is a pointillistic SR method that uses fluorophores which are photoactivable [5,6]. These fluorophores require radiation from an activation light before they can be put into an excited state by the excitation light and are packed denser than the resolution limit in the sample. In PALM, the intensity of this activation light is chosen such that fluorophores that are within a resolvable distance are activated. The fluorophores are then excited and localized via an algorithm. The process is repeated until all the fluorophores have been imaged. From the stack of images acquired a composite image is constructed. The limits to the resolution are determined by the SNR of single fluorophore emission via the localization precision, which is limited by the maximal number of photons a single fluorophore can emit before bleaching. Additionally, it is not possible to determine how many frames are needed to create the SR image since each sample will have a different number of fluorophores excited per exposure depending on the local chemical environment. PALM is best suited for structures that are static with low density. Structured illumination microscopy (SIM) is a widefield method that purposefully undersamples the object so that high frequency components of the object are brought into low frequency space by interference [7,8]. A superresolution image is constructed from multiple full field exposures under changing structured illumination phase. Measuring this phase is a challenge and error in measurement introduces artifacts in

the final image. The structured illumination (SI) can be either an activation or a quenching effect. An effect which has a linear dependence on photons activated or quenched depending on SI intensity is capable improving the resolution by a factor of two. An effect which has a nonlinear dependence between the SI and the number of photons emitted is theoretically unlimited in its ability to enhance the resolution. There are four main effects used for nonlinear SIM: excitation saturation, photoswitching depletion, photoactivation, and Stimulated Emission Depletion (STED) [9]. Excitation saturation uses a high intensity that accelerates fluorophore bleaching. All four of these effects are limited by the photon budget and the labeling density which effects the image quality. A common structured illumination pattern results from the interference of two laser beams. In the SIM image reconstruction algorithm, past work often assumes that the two beams are plane waves which leads to an interference illumination with uniform periodicity [10]. But the assumption is never true even in an ideal imaging system. When the interference pattern is formed from laser beams, the beam shape is better modeled as Gaussian than a plane wave. This is because a finite pupil size causes diffraction of the beam so that it is never a plane wave. The interference of two tilted Gaussian beams produces an illumination field that has nonuniform spacing between the fringes. In addition, optical aberration will further distort fringes. I will show that these aberration effects lead to artifacts in the superresolution image. I will also outline a way to construct the superresolution image without these artifacts based on the abundance of information contained in SIM raw images.

## Chapter 2: The Theory of SIM

SIM has the largest potential user base amongst biologists. This is because the method is capable of near 50 nm resolution at a time scale of seconds and does not require special fluorophores like STED and PALM. Well known microscopy companies are releasing linear SIM microscopes and even microscopes that can improve the linear SIM resolution by a factor of two at the time of this writing. SIM though does not necessitate the use of fluorophores. Any object that produces or inhibits photons with a nonlinear response from the structured illumination holds potential [11].

A quenching effect with nonlinear behavior is a photo emission effect which is ideal for SIM since it will improve the Signal to Noise Ratio (SNR). The SNR of a fluorescence signal follows a  $\sqrt{N}$  relation where  $N$  is the number of photons for the case of nonlinear effects that are based on photon emission and  $N$  is the fluorophore density for the case of nonlinear effects which depend on photoswitching. This means that a nonlinear effect based on photoswitching is improved upon based on the chemistry of dyes rather than any fundamental physics. In a system that uses STED as the quenching effect an excitation beam,  $I_{ex}$ , is first applied to the fluorophore distribution,  $\rho$ , followed by the quenching beam,  $I_q$ . The SIM process purposefully undersamples  $\rho$ . In Fourier space the effect of  $I_q$  on the  $\rho$  is to convolve a series of Dirac deltas with  $\rho(k)$  which brings high frequency information into the passband of the imaging system. The interaction of the excitation and quenching beams follows  $I_{int} \propto I_{ex} / I_q$ . It can be shown that quenching has this effect based on a Taylor series expansion of the emission intensity which is given as

$$I_{em}(\rho(x), I_{int}(x)) = c_0 + c_1\rho(x) + c_2\rho(x)I_{int}(x) + c_3\rho(x)I_{int}(x)^2 + c_4\rho(x)I_{int}(x)^3 \quad (3)$$

I have assumed that the  $\rho$  follows a linear dependence on the excitation. I will simplify the emission equation and show its Fourier space equivalent by ignoring constant offsets to

$$I_{em}(x) = \rho(x) \sum_i^{\infty} c_i I_{int}(x)^i \iff I_{em}(k) = \rho(k) \otimes \sum_i^{\infty} c_i I_{int}(k)^i \quad (4)$$

(2.2) The optical imaging system further multiplies the Fourier space emission equation by an optical transfer function. The  $c_i I_{int}(k)^i$  terms of the emission will be Dirac deltas when the structured illumination is sinusoidal. Each of these Diracs brings some of the high frequency information into the low frequency passband of the imaging system. Shifting the phase of the structured illumination results in shifting the position of the Dirac deltas thus putting more high frequency information into low frequency space. This is equivalent to expanding the OTF by the circles as shown in figure 1a. We need information from at least three phases shifts within one revolution of the unit circle to create an image with enhanced resolution by a factor of two. Enhancing the resolution further is possible by introducing more phases shifts within the unit circle and at the same time increasing the nonlinear strength so that more terms in the summation of equation are above the noise floor. We start to run into noise issues at a certain increase in nonlinearity and diffraction at a certain increase in phase shift density. It is easiest to understand how to put the down modulated information back into high frequency space for the final image by looking at the case of  $i = 1$ . In this case we shift each phase dependent image by an amount  $k$  corresponding to the phase shift in Fourier space. In practice this shift should be done in real space by a complex exponential since  $k$  mostly likely will be a non-integer value in the discrete Fourier space. Conceptually we stay in Fourier space and consider that the shift puts each image into a different position in Fourier space as shown in figure 1b. In the literature theorists cite that an apodization can then be performed and any filtering to display the information once it is transformed back into the spatial domain [12].

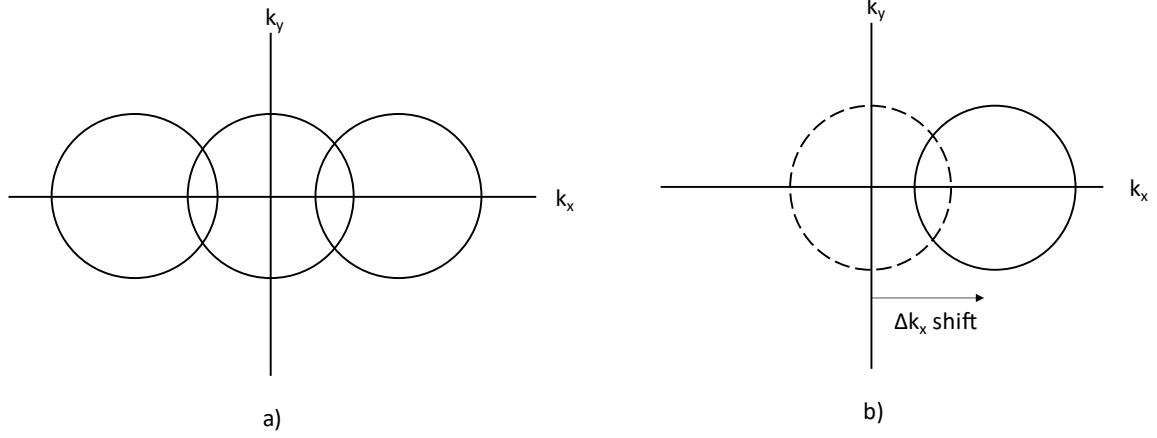


Figure 1: a) 1D Linear SIM patches in frequency domain and b) 1D linear SIM patch frequency shift where the dotted circle is the original location, and the solid circle is the frequency shifted location

### Chapter 3: Aberration Correction Theory and Simulation

This thesis simulates a target in 1D SIM, adds aberration effects to the structured illumination and then corrects the aberration effects. The idea with the correction is to apply a low pass filter to the data to get information about the variation of the structured illumination. The low pass filter is applied to the reconstructed data and then the data is reconstructed again with a new term introduced into the reconstruction matrix [13]. The variation is a function of the spatial dimension(s) that the structured illumination exists in. For 1D SIM the variation function is the phase function  $\psi(x)$ . The matrix is looped over the x and y dimensions so that there is a three-by-three matrix for each pixel.

The MATLAB code is structured in three scripts. The script for creating the raw data is setup as a class with functions that belong to that class. An example is the planewave gaussian envelope function which is:

```
function [I,X,phase,x] = planewave_SI_withgaussianenvelope(pixels,fringe_spacing,N,I_STED,dimensions)
    x = linspace(-1,1,pixels);
    [X,Y] = meshgrid(x,x);
    phase = 2*linspace(0,2*pi,N)/N;
    A = 1;
    theta = 60;
    B = A/cosd(theta)
    for c=1:N
        I(:,:,c) = exp(-(X.^2)/(B^2)+(-
            (Y.^2)/A^2)).*sin((X/fringe_spacing)+phase(c))+1;
    end
end
```

The script for creating the superresolution images consists of one function. One example in the reconstruction is the matrix:

```
%Calculate M, M is for separating the orders
index_M = linspace(1,N,N);
index_M_transpose = index_M.';
index_M_matrix = index_M.*index_M_transpose;
M = exp(1j*2*pi*index_M_matrix./N);
M_inverse = inv(M);
```

The script for running all three scripts sets the constants, calls the functions in the raw data class and runs the superresolution script. One example of calling a function is the emission:

```
E = STEDSIM_simulation_raw_data_functions.emission(I,S_array);
```

There are computational reasons why some functions cannot be implemented in the simplest physical model possible. One of the challenges in the computer code was how to properly form the structured illumination. The simplest physical way to form the structured illumination is to have two gaussian beams at the back focal plane and Fast Fourier Transform (FFT) to the front focal plane. The problem with implementing this computationally is that the Gaussian beams will be smaller than the resolution size so they will only take up a few pixels thus eliminating the Gaussian information and instead be like Dirac deltas. This means that the structured illumination will not include the Gaussian information. The solution to this challenge is to write into the code the geometry of the structured illumination directly at the front focal plane. The simplest way to do this is to have a plane wave geometry with a Gaussian envelope which assumes that the Gaussian beam is cylindrical. Another challenge in the computer code with a similar root problem is with the point spread function of the system. It too shows up as only a few pixels when implemented directly as a point spread function and using FFT to form the OTF. The solution is to have an analytical function of the OTF instead of computing it from the FFT.

The simulation has a field of view of 10.24 microns and the widefield image without the OTF has a resolution of 10 nm/pixel. The OTF has a maximum frequency set by the resolution of  $\lambda$  over two NA which is 247 nm in terms of the spatial domain. The wavelength of the emission is 650 nm, and the NA is 1.31562. The phase of the structured illumination varies from zero to two  $\pi$  with three phase steps. The superresolution image shows a twofold improvement in the resolution. The simulation could improve the resolution further by using nonlinear SIM. It will be shown that the aberration correction method works well enough to correct aberrations.

The process to form the raw data images in the code consists of several steps. The first step is to

create the object. This is done using the function from the LP paper 2020 [13]. This object is created into an array of matrices set by the number of orders needed which for linear SIM is only the first order so three instances of matrices are needed. The next step is to create the structured illumination. This is done analytically at the front focal plane where the two Gaussian beams intersect at the sample. For diagnostic purposes the structured illumination array is summed to check if it adds up to a uniform illumination which it does when the structured illumination is made correctly. The next step is to define the optical transfer function analytically using the constants of wavelength and NA as scaling factors. The emission pattern is then formed by the element-wise multiplication of the structured illumination with the object array. The final step to create the raw data frames is element-wise multiplication of the FFT of the emission with the OTF and inverse FFT of each frame.

The target for the simulation is a wheel of spokes. This target was chosen because of its symmetry and its gradual change from wider to narrower in the outer pixels to the inner pixels. The target is shown in figure 2 along with the sum of the raw data. The sum of the raw data includes the effects of the OTF and the structured illumination at all three phases.

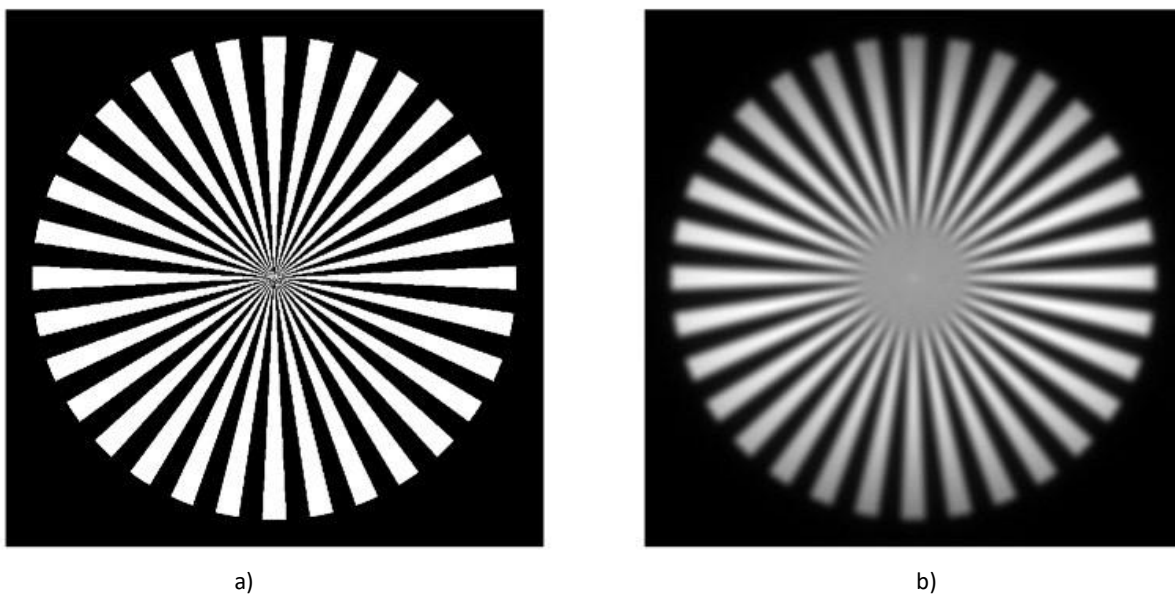


Figure 2: a) Simulated target b) Sum of raw data taken at all phases of structured illumination

The blur in the center of the raw data is due to the OTF and no effects of aberrations can be seen in the raw data in the cases where there are aberration effects in the structured illumination and in the cases where there are no aberration effects in the structured illumination. The SIM superresolution image can be displayed as the sum of the first orders alone or include the zero order in the sum. The reason it can be helpful to sum just the orders is because the zero order has greater intensity than the orders so that in some cases subtle visual details are not as easy to observe with the zero order included. Figure 3 shows the superresolution image with and without the zero order with an ideal structured illumination.

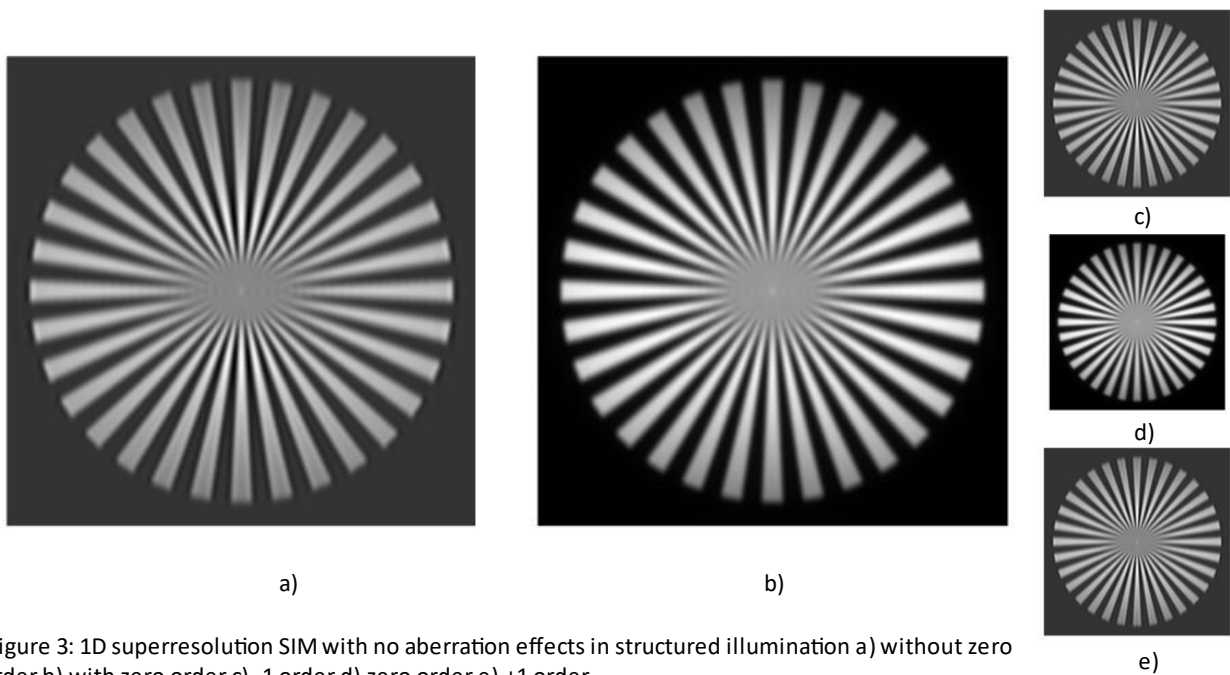


Figure 3: 1D superresolution SIM with no aberration effects in structured illumination a) without zero order b) with zero order c) -1 order d) zero order e) +1 order

The symmetry of the algorithm results in the plus one order and minus one order looking indistinguishable (figure 3 c and 3 e). The center area of the superresolution image has some periodic artifacts.

When one wave of aberration effects is introduced into the structured illumination the superresolution image becomes distorted as shown in figure 4.

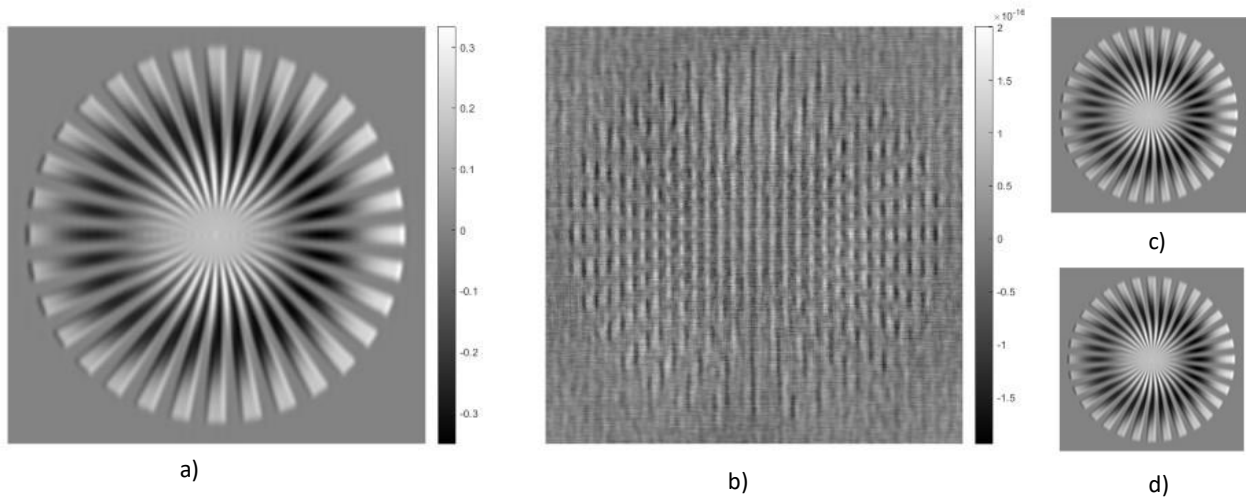


Figure 4: 1D Superresolution SIM with 1 wave aberration effects and no zero order, a) real and b) imaginary components c) real -1 order d) real +1 order

The distortion in the structured illumination was created by a Zernike phase map. Figure 4 shows the intensity of the superresolution image in real space and imaginary space. The real space is non-zero valued and the imaginary space is essentially zero valued. Again, there is symmetry in the individual orders.

The code for superresolution formation extracts high frequency information and shifts it to the proper place in the frequency domain and then sums the orders. The code first takes the FFT of the raw data frames and calculates the matrix for solving the orders. This is done by creating an index, matrix multiplying it by its transverse, taking the complex exponential of the index matrix and then its inverse. The next step is to take the IFT of the solved frames to prepare for the frequency shift which is done in the spatial domain rather than in the frequency domain. To do this the code first sets up the frequency shift by defining the range over the dimension that it will occur, the order values and the fringe spacing. Next, the solved data frames are element-wise multiplied in the corresponding dimension by the complex exponential with a period given by the fringe spacing. An extra section of the code in this script is for matching the phase between orders which is not used in linear SIM but is used in nonlinear

SIM. The final step to create the superresolution image is to take the absolute value of each frame and then sum all frames together. The image of the phase map is shown in figure 5 with a scalebar. This phase map is what causes the aberrated effects in the structured illumination.

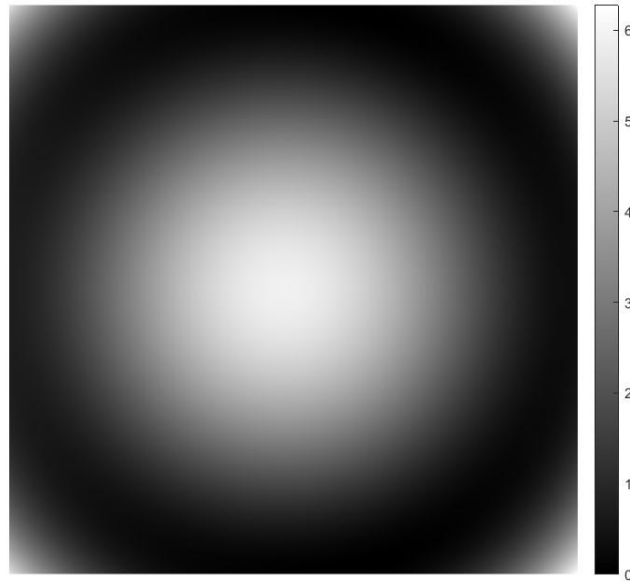


Figure 5: 1 wave phasemap for creating aberration effects generated from Zernike polynomials

The scale of the phase map is an independent variable which can be changed to show waves of distortion such as 0.5 waves, 1 wave or 2 waves. The phase map is generated from Zernike polynomials and involves spherical, coma and astigmatism associated polynomials. For the purpose of this research, it is not relevant what the specific aberrations are since the correction algorithm is aberration type independent.

Figure 6 shows the 1D structured illumination distorted by 0.5,1, and 2 wave phase maps.

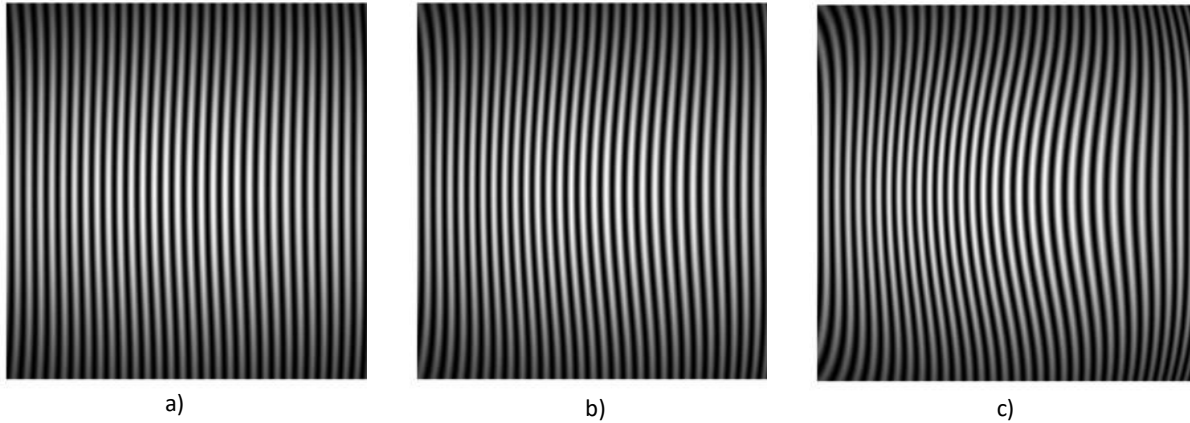


Figure 6: 1D Structured illumination a) 0.5 wave, b) 1 wave, and c) 2 wave distortion

The distortion is observable as bends in all three images and is in a range that similar enough to experimental conditions.

The correction function part of the code has two main aspects. The calculation of the correction function  $\psi(x)$  and its implementation in the reconstruction. The first part is to set the constants for the low pass filter. The low pass filter is implemented as an OTF. The wavelength is used, and the difference is found between the one over resolution and one over the fringe period. The NA of the OTF is found by multiplying this difference by wavelength divided by two and using a scale factor of 0.8. This implementation of the OTF consists of using these parameters with the analytical OTF. The frames are next FFTed to the Fourier domain and multiplied by the OTF as a low pass filter elementwise then inverse FFTed back to the spatial domain. The  $\pm 1$  orders are then summed, and the MATLAB angle function is used to get the complex phase which is  $\psi(x)$ .

The superresolution image with aberration effects is corrected by first gaining back the phase map information through low pass filtering of the superresolution image. The pupil function which is four dimensional  $(x, y, P_x, P_y)$  for these aberration effects essentially consists of two points which are in

fact two small areas where the Gaussian beams are. It is the difference in the aberrations between these two areas that leads to the aberration effects in the structured illumination. There are similarities and differences to how this is done with light sheet imaging [13]. The biggest difference is regarding the maximum frequency of the structured illumination. In light sheet SIM the maximum frequency of the structured illumination is not close to the diffraction limit. In the case of superresolution SIM, it is. This difference is illustrated in figure 7. Consequently, the space available for the lowpass filter in lightsheet SIM is larger than in superresolution SIM.

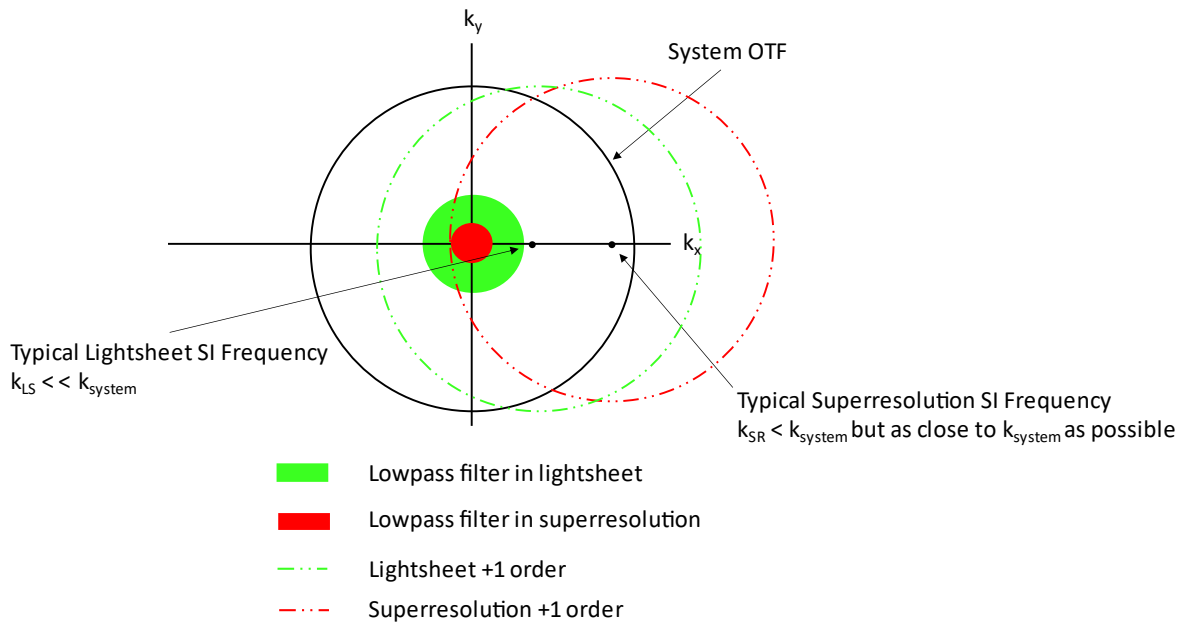


Figure 7: Comparison of lightsheet and superresolution structured illumination.

Additionally, it is assumed that  $\psi(\mathbf{x})$  is slowly varying compared to the size of the PSF. The intensity equation is:

$$I(\vec{x}, \phi_m) = \sum_n a_n \exp(in\phi_m) \times \{O(\vec{x}) \exp(in\vec{x} \cdot \vec{k}_0) \exp(in\psi(\vec{x}))\} \otimes PSF(\vec{x}) \quad (5)$$

Where

$$\phi_m = \frac{2m\pi}{2N+1} + \vec{k}_0 \cdot \vec{x} \quad (6)$$

$\psi(\mathbf{x})$  is slowly varying so equation 5 becomes:

$$I(\vec{x}, \phi_m) \approx \sum_n a_n \exp(in\phi_m) \times \{O(\vec{x}) \exp(in\vec{x} \cdot \vec{k}_0) \otimes \text{PSF}(\vec{x})\} \times \exp(in\psi(\vec{x})) \quad (7)$$

Which means that the matrix  $\mathbf{M}$  becomes:

$$\mathbf{M}(\vec{x})_{nm} = \exp(inm \frac{2m\pi}{2N+1}) \exp(in\psi(\vec{x})) \quad (8)$$

These equations are from [13]. Figure 8 shows the recovered phase map information from the

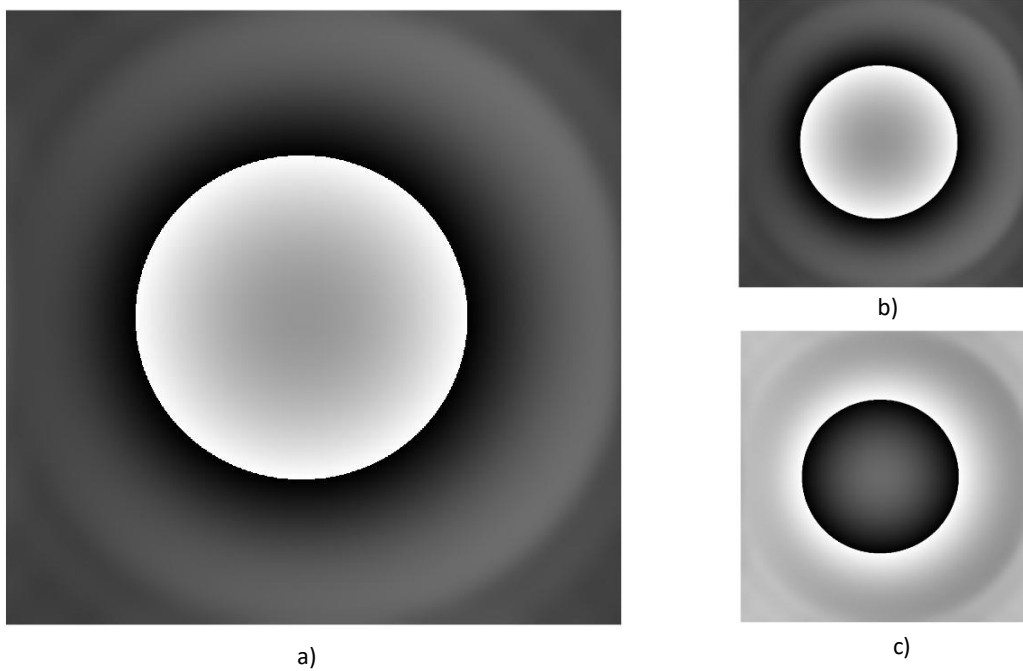


Figure 8: Recovered phasemap a) 1 wave summed b) 1 wave -1 order c) 1 wave +1 order

superresolution image with one wave aberration effects. The phase information is in the wrapped condition in these images. Unwrapping the phase information using a MATLAB function freely available on the internet produces a recovered phase map like the original phase map as shown in

figure 9. In both cases the plus one and negative one orders that the phase map is composed of are conjugates.

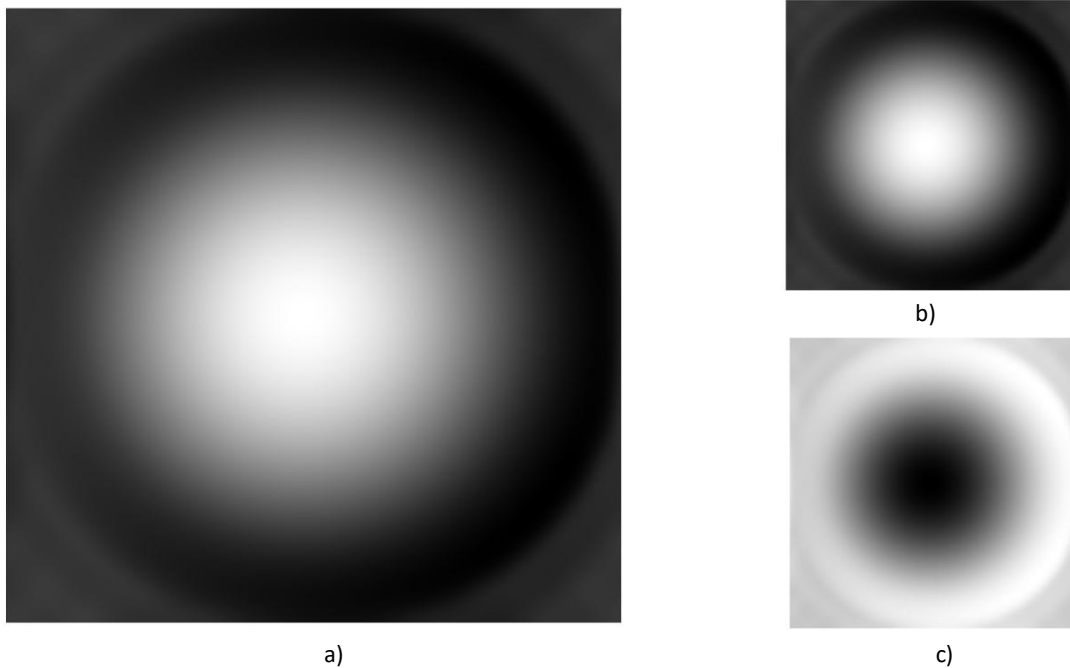
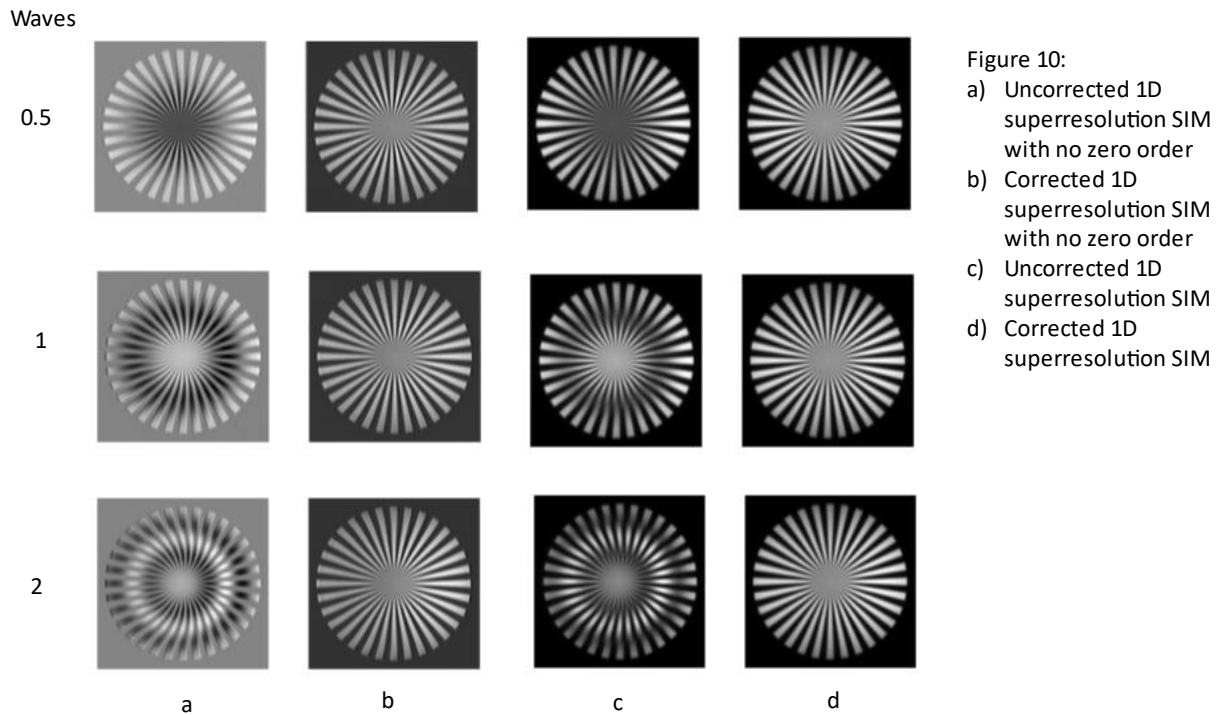


Figure 9: Unwrapped Recovered phasemap a) 1 wave summed b) 1 wave -1 order c) 1 wave +1 order

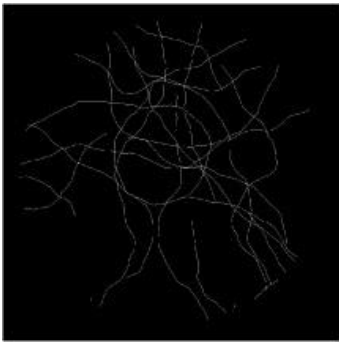
The reconstruction process follows a similar process as before but this time the matrix for solving the frames involves  $\psi(x)$ . To do this the matrix is multiplied by the complex exponential of  $n$  times  $\psi(x)$  where  $n$  is the order. The inverse is made by dividing with the MATLAB backslash operator since the inverse function gives a singular matrix. The solving of the orders is implemented as before and so is the frequency shift. The frames are summed together to form the corrected superresolution image.

The simulation results for 0.5, 1, and 2 wave structured illumination aberration effects are shown in figure 10 in the case of without the zero order and in the case with the zero order. In every condition the corrected superresolution shows clearly visible aberration effect correction.

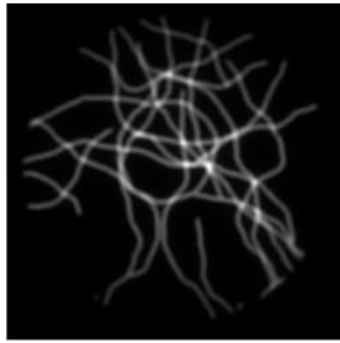


As the number of waves in the aberration effects increases to two waves intensity non-uniformity is prevalent even in the corrected image.

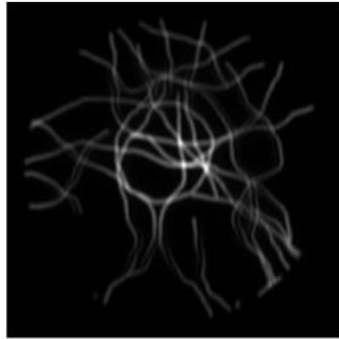
It is possible to simulate a different target such as a random fiber target. Figure 11 shows the results of a random fiber target with one wave aberration effects in the structured illumination. The superresolution image shows distortion on some of the vertical fibers such as the ones in the lower right quadrant. These distortions are corrected in the corrected superresolution image.



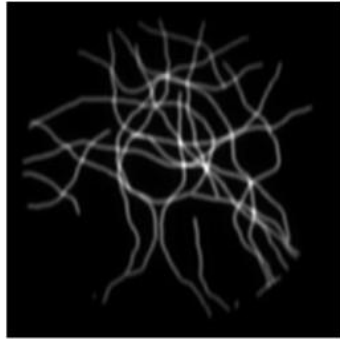
a)



b)



c)



d)

Figure 11:

- a) Simulated random fiber target
- b) Sum of raw data taken at all phases of structured illumination
- c) 1D SIM superresolution 1 wave aberration effects
- d) Corrected 1D SIM superresolution 1 wave aberration effects

## **Chapter 4: Conclusions and Future Work**

This thesis overviewed methods for improving resolution, described the theory of SIM and then presented a superresolution SIM computer simulation. The results show that the code can be used to form a 1D superresolution SIM image. The data also shows that the aberration correction method works in 1D superresolution SIM with both a spoke target and a random fiber target. The code was implemented computationally differently than the theoretical model because of the pixel size needed for the structured illumination and the PSF. Setting up the code into different scripts with function definitions and class structure made different parts of the code easy to reuse. This research has extended on a paper [13] where an aberration effect correction was implemented in lightsheet SIM by using the same theory. Future work could consist of increasing the number of dimensions that the superresolution occurs in and increasing the number of orders from linear to nonlinear SIM. Another aspect of future work could be experimentally verifying the aberration correction method.

## Appendix

Raw data functions script:

```
classdef STEDSIM_simulation_raw_data_functions
    methods (Static)

        function object = object_spokes (pixels, SpokeNumber, PatternNumber) %This
function is from LP
        [x, y] = meshgrid((1:pixels)/pixels*2-1, (1:pixels)/pixels*2-1);
        r = sqrt(x.^2+y.^2);
        theta = angle(x+1i*y);
        SubTarget = +(mod(round((theta+pi)/pi*SpokeNumber),2)<1);
        SubTarget(r>0.9)=0;
        object = zeros(pixels)*PatternNumber;
        for ii = 1:PatternNumber
            for jj = 1:PatternNumber
                object((1:pixels)+(ii-1)*pixels, (1:pixels)+(jj-1)*pixels) =
SubTarget;
            end
        end
    end
end

% function [I,X,phase,x] = planewave_SI (pixels, fringe_spacing, N, I_STED, di-
mensions)
%     x = linspace(0,3*pi,pixels);
%     [X,Y] = meshgrid(x,x);
%     %phase = exp(1j*linspace(0,2*pi,N));
%     phase = linspace(0,2*pi,N)/N;
%     for c=1:N
%         I(:, :, c) = sin((X/fringe_spacing)+phase(c))+1;
%     end
% end

function [I,X,phase,x] = planewave_SI_withgaussianenvelope (pixels, pe-
riod, N, dimensions, phasemap)
    x = linspace(-1,1,pixels);
    [X,Y] = meshgrid(x,x);
    phase = 2*linspace(0,2*pi,N)/N;
    A = 1;
    theta = 60;
    B = A/cosd(theta);
    if exist('phasemap','var')
        for c=1:N
            I(:, :, c) = exp(-(X.^2)/(B^2)+(-(Y.^2)/A^2)).*(cos(2*pi*X/(2*pix-
els*period)+phase(c)+phasemap)+1);
        end
    else
        for c=1:N
            I(:, :, c) = exp(-(X.^2)/(B^2)+(-(Y.^2)/A^2)).*(cos(2*pi*X/(2*pix-
els*period)+phase(c))+1);
        end
    end
end

function [phasemap,indexforvector]= phasemapfun (pixels)
    n = [4 3 2];
    m = [0 1 2];
```

```

amp = [1,7,1]; %adjust amp
x = linspace(-1,1,pixels);
[X,Y] = meshgrid(x,x);
[theta,radii] = cart2pol(X,Y);
radii = radii/sqrt(2);
indexforvector = radii<=1;
phasemap = zeros(pixels);
for c = 1:length(n)
    zf = zernfun(n(c),m(c),radii(indexforvector),theta(indexforvector));
    phasemap(indexforvector) = amp(c)*phasemap(indexforvector) + zf;
end
phasemap(indexforvector) = (phasemap(indexforvector)-min(phasemap(indexforvector)));
phasemap(indexforvector) = phasemap(indexforvector)/(max(phasemap(indexforvector))-min(phasemap(indexforvector)));

waves = 1;
phasemap(indexforvector) = waves*2*pi*(phasemap(indexforvector));
end

% function [I,Ix] = planewave_SI_square(pixels,fringe_spacing,N,I_STED)
%     pixels = 1024;
%     period = 1;
%     number_of_periods = 10;
%     unit_rect_ones = 1;
%     preI= zeros(1,3,3);
%     for c=1:3
%         preI(1,c,c) = 1;
%     end
%     preI = repmat(preI,1,number_of_periods);
%     for c=1:3
%         [Ix(:,:,c),Iy(:,:,c)] = meshgrid(preI(:,:,c),preI(:,:,c));
%         I(:,:,c) = imresize(Ix(:,:,c), pixels/length(preI));
%     end
%     end

function S_array = object_array(S,N)
    S_array = repmat(S,1,1,N);
end

% function gauss_pair_2D_array = gauss_pair(origin_offset,diameter,phase,
one_over_f, xline,yline,N,pixels)
%     %gauss pair function
%     gauss_pair_2D_array = zeros(pixels,pixels,N); %the gaussian beams are
at the beam waist, calc NA of SI using distance between beams
%     for c=1:N
%         gauss_pair_2D_array(:,:,c) = exp(-one_over_f.*(((xline-origin_offset)./diameter).^2)+((yline)./diameter).^2)).*exp(1j.*phase(c))+exp(-one_over_f.*(((xline+origin_offset)./diameter).^2)+((yline)./diameter).^2));
%     end
%     end

% %SI function
% function I = SI(gauss_pair_2D_array, I_STED, N)
%     %Lens transform
%     u = gauss_pair_2D_array;
%     for c=1:N

```

```

%         u(:,:,c) = fftshift(fft2(u(:,:,c)));
%     end
%     %Irradiance
%     I= abs(u).^2;
%     for c=1:N
%         I(:,:,c) = rescale(I(:,:,c));
%     end
%     %STED
%     I = 1./(1+I_STED*(0.5+0.5*I)); %The same as with the cos pattern but
now the I put in has a gauss envelope
%     end

function save_SI(I, filepath)
%Save SI function
writematrix(I,filepath,'Delimiter',' ');
end

function otf = otf_function(pixels,wavelength,NA)
resln = wavelength/(2*NA);
%x = (1:pixels)/pixels*2-1;
x = (0:(pixels-1))/pixels*2-1; %for having single pixel max and chang-
ing location to 513,513
y = (0:(pixels-1))/pixels*2-1;
[X,Y] = meshgrid(x,y.' );
radii = resln*sqrt(X.^2 +Y.^2)/(2*sqrt(2));%factor of two based on
guess, sqrt 2 to norm to 1
otf = real(2/pi*(acos(abs(radii))-abs(radii).*sqrt(1-radii.^2)));
end

function E = emission(I,S_array)
%Emission function
%Emission rate distribution
E = I.*S_array;
end

function [D,E_fft,ft_D] = data(E,pixels,OTF)
%Data function
%Convolution of emission rate distribution with PSF
%Observed data, D, as the convolution of the emission rate distribution
with the PSF
%preallocate array outside of for loop
E_fft = fftshift(fft2(E));
D = zeros(pixels,pixels,size(E,3));
for c=1:size(E,3)
    ft_D(:,:,c) = E_fft(:,:,c).*OTF;
    D(:,:,c) = ifft2(ifftshift(squeeze(ft_D(:,:,c))));
end
end

function save_data(S,E,D, filepathS, filepathE, filepathD)
%Save data function
writematrix(S,filepathS);
writematrix(E,filepathE);
writematrix(D,filepathD);
end
end
end

```

## Create Superresolution Images Script:

```
function [M,SR,ft_D,M_inverse,S_solved,S_ifft,...
    ft_S_ifft_k_shift,S_ifft_k_shift, shift_phase_factor_x, Widefield_wo_psf,Wide-
field_w_psf, ...
    psi_x,calpsiS_solved_lowpass, CorrSR, otflp,...
    NA_lp,CorrS_k_shift,CorrS_solved] = STEDSIMsimulation_create_superresolution_im-
ages(n,N,D,E,pixels, dimensions,OTF,period,ft_D,pixelsize,NA)

%Calculate M, M is for separating the orders
index_M = linspace(-1*(N-1)/2, (N-1)/2,3);
index_M_transpose = index_M.';
index_M_matrix = index_M.*index_M_transpose;
M = exp(1j*2*pi*index_M_matrix./N);
M_inverse = inv(M);

%Get the solved linear equation frames, does not reverse FT or k shift.
S_solved_n = zeros(pixels,pixels);
S_solved = zeros(pixels,pixels,N);
for c2=1:N
    S_solved_n = zeros(pixels,pixels,N);
    for c1=1:N
        S_solved_n(:, :,c1) = ft_D(:, :,c1).*M_inverse(c2,c1,1);
    end
    S_solved(:, :,c2) =
S_solved_n(:, :,1)+S_solved_n(:, :,2)+S_solved_n(:, :,3); %for linear SIM, need to
change for nonlinear
end

%Take the IFT of the solved frames
%S_ifft = zeros(pixels,2*(pixels),N);
for c=1:N
    S_ifft(:, :,c) = ifft2(ifftshift(S_solved(:, :,c))); %Removed additional fftshift
when using OTF
end

%k shift the solved frames
x = linspace(-1,1,pixels);
fringe_spacing = period*2/pixels;

n = (N-1)/2:-1:-(N-1)/2;

for c=1:N
    n_times_x(:,c) = n(c).*x;
end
%k_x shift
shift_phase_factor_x = exp(1j*n_times_x.*(2*pi/fringe_spacing)); %No y for 1d
%S_ifft_k_shift = zeros(pixels,N*pixels,2*N);
for c1 = 1:N
    for c3 = 1:pixels
        S_ifft_k_shift(:,c3,c1) = S_ifft(:,c3,c1).*shift_phase_fac-
tor_x(c3,c1);
    end
end

ft_S_ifft_k_shift = fftshift(fft2(ifftshift(S_ifft_k_shift)));
ft_S_ifft_k_shift_01 = ft_S_ifft_k_shift(:, :,1);

SR = S_ifft_k_shift(:, :,1)+S_ifft_k_shift(:, :,2)+S_ifft_k_shift(:, :,3);
% SR = S_ifft_k_shift(:, :,1)+S_ifft_k_shift(:, :,3);
```

```

Widefield_wo_psf = abs(E(:,:,1)+E(:,:,2)+E(:,:,3));%Can use this to find out if
problems are in forming the SI images or the SR image
Widefield_w_psf = abs(D(:,:,1)+D(:,:,2)+D(:,:,3));

%Calculate psi_x using lowpass filter
wavelength = 650*(1/pixelsize); %nm*pixel/nm
resolution = wavelength/2/NA;
lpcutoff = 1/resolution-1/period;
NA_lp = lpcutoff*wavelength/2*0.8;
pixels = 1024;
otflp = STEDSIM_simulation_raw_data_functions.otf_function(pixels,wave-
length,NA_lp);

for c=1:N
    calpsiS_solved_lowpass(:,:,c) =
fftshift(iff2(iffshift(ft_S_ift_k_shift(:,:,c).*otflp))); %Use OTF of deltaNA
end
psi_x = (angle(calpsiS_solved_lowpass(:,:,1))-angle(calpsiS_solved_low-
pass(:,:,3)))/2;

%%
%need to loop over x and y so that there is a matrix for each pixel
%Reconstruct with psi_x
for c2=1:pixels
    for c1=1:pixels
        M_wpsix = exp((1j*2*pi*index_M_matrix./N)+1j*n*psi_x(c1,c2));
        CorrS_solved(c1,c2,:) = M_wpsix\squeeze(D(c1,c2,:));
    end
end

%Take the IFT of the solved frames
%k_x shift
for c1 = 1:N
    for c3 = 1:pixels
        CorrS_k_shift(:,c3,c1) = CorrS_solved(:,c3,c1).*shift_phase_fac-
tor_x(c3,c1);
    end
end

CorrSR = CorrS_k_shift(:,:,1)+CorrS_k_shift(:,:,2)+CorrS_k_shift(:,:,3);
% CorrSR = CorrS_k_shift(:,:,1)+CorrS_k_shift(:,:,3);
%%

%Save images
writematrix(SR,"SR.dat");
writematrix(Widefield_wo_psf,"Widefield_wo_psf.dat");
writematrix(Widefield_w_psf,"Widefield_w_psf.dat");

%Show images
figure()
nexttile()
imshow(Widefield_wo_psf,[]),title('Sum of Emission')
nexttile()
imshow(Widefield_w_psf,[]),title('Sum of Raw Data')
nexttile()
imshow(real(SR),[]),title('SR')
nexttile()

```

```

imshow(real(CorrSR),[]),title('CorrSR')

figure(),imshow(CorrSR,[])

%figure(),nexttile(),imshow(SR,[]),nexttile(),imshow(CorrSR,[])

```

end

### Automate Simulation Script:

%Define the physical parameters used in the formation of an object for STED-SIM and in the formation of a SR image.

```

clear;
tic;
%Object
pixels = 1024;
SpokeNumber = 32;
PatternNumber = 1;

pixelsize = 10; %nm
totalpixelsize = pixelsize*pixels; %nm

%Beams
NA_emission = 1.49;
%pulse_duration = 200; %pS
%structured illumination
%STED_power_at_sample = 9; %mW
%STED_field_size = 12; %micron^2 e^2 diameter
%NA_STED = 0.92;
n = 1; %1 is linear SIM, >1 nonlinear SIM
N = 2*n+1;
%I_STED = 8;
%SI_periodfactor = 1/pixelsize;
%excitation
%excitation_power = 1; %mW
%excitation_size = 24; %micron^2 e^2 diameter
%lens
%one_over_f = linspace(0.5,1.5,10);%prop to NA
%one_over_f = 1; %Units?
%H = 1;%?
%Gaussian Beam
%make one_over_f multipliable by the phase
%one_over_f = one_over_f(:,:,:);
%Define gaussian functions on a 2D array of zeros
x = linspace(-1,1,pixels);
%x= 1:1:pixels;
[X,Y] = meshgrid(x,x);
xline = X;
yline = Y;
phase = linspace(0,2*pi,N)/N;
%diameter = 1/(10^3); %sets gaussian envelope
%origin_offset = 200/(10^4); %sets number of fringes, units?

%NA_SI = origin_offset/1; %?just origin_offset.5;
PatternPeriod = 320/pixelsize; %320 nm;
wavelength = 650*(1/pixelsize); %nm*(1pixel/xnm)
NA = wavelength/2/PatternPeriod+0.3;

```

```

%SR Image
dimensions = 1;
R = 2*430/(N+1);

S = STEDSIM_simulation_raw_data_functions.object_spokes(pixels, SpokeNumber, PatternNumber);
load Target1024.mat; %Random fiber target
S = Target;
S_array = STEDSIM_simulation_raw_data_functions.object_array(S,N);
%gauss_pair_2D_array = STEDSIM_simulation_raw_data_functions.gauss_pair(origin_offset,diameter,phase, one_over_f, xline,yline, N,pixels);
%I = STEDSIM_simulation_raw_data_functions.SI(gauss_pair_2D_array, I_STED, N);
%I = STEDSIM_simulation_raw_data_functions.planewave_SI(pixels,fringe_spacing,N,I_STED,dimensions);
[phasemap,indexforvector] = STEDSIM_simulation_raw_data_functions.phasemapfun(pixels);
I = STEDSIM_simulation_raw_data_functions.planewave_SI_withgaussianenvelope(pixels,PatternPeriod,N,dimensions,phasemap);
Sum_SI = I(:, :, 1)+I(:, :, 2)+I(:, :, 3);
%I = aberrSI; %for aberrrated SI
OTF = STEDSIM_simulation_raw_data_functions.otf_function(pixels,wavelength,NA);
% STEDSIM_simulation_raw_data_functions.save_SI(I, "I.dat");
E = STEDSIM_simulation_raw_data_functions.emission(I,S_array);
[D,E_fft,ft_D] = STEDSIM_simulation_raw_data_functions.data(E,pixels,OTF);
% STEDSIM_simulation_raw_data_functions.save_data(S, E,D, "S.dat", "E.dat", "D.dat");
%%
[M,SR,ft_D,M_inverse,S_solved,S_ift,...
ft_S_ift_k_shift, S_ift_k_shift, shift_phase_factor_x,...
Widefield_wo_psf,Widefield_w_psf,psi_x,calpsiS_solved_lowpass, CorrSR, otflp,NA_lp,CorrS_k_shift,CorrS_solved] =...
STEDSIMsimulation_create_superresolution_images(n,N,D,E,pixels,dimensions,OTF,PatternPeriod,ft_D,pixelsize,NA);
%%
Total_time = toc/60; %Minutes

```

## References

- [1] W. Lukosz and M. Marchand. Optischen Abbildung Unter Überschreitung der Beugungsbedingen Auflösungsgränze. *Optica Acta: International Journal of Optics*, 10(3):241–255, July 1963.
- [2] W. Lukosz. Optical systems with resolving powers exceeding the classical limit. *JOSA*, 56(11):1463–1471, 1966.
- [3] Harootunian, A., Betzig, E., Isaacson, M., & Lewis, A. (1986). Super-resolution fluorescence near-field scanning optical microscopy. *Applied Physics Letters*, 49(11), 674-676.
- [4] Hell, S. W., & Wichmann, J. (1994). Breaking the diffraction resolution limit by stimulated emission: stimulated-emission-depletion fluorescence microscopy. *Optics letters*, 19(11), 780-782.
- [5] Betzig, E., Patterson, G. H., Sougrat, R., Lindwasser, O. W., Olenych, S., Bonifacino, J. S., ... & Hess, H. F. (2006). Imaging intracellular fluorescent proteins at nanometer resolution. *science*, 313(5793), 1642-1645.
- [6] Ulrike Endesfelder and Mike Heilemann. Art and artifacts in single molecule localization microscopy: beyond attractive images. *Nature Methods*, 11(3):235–238, March 2014.
- [7] Neil, M. A., Juškaitis, R., & Wilson, T. (1997). Method of obtaining optical sectioning by using structured light in a conventional microscope. *Optics letters*, 22(24), 1905-1907.
- [8] Heintzmann, R. (2003). Saturated patterned excitation microscopy with two-dimensional excitation patterns. *Micron*, 34(6-7), 283-291.
- [9] Gustafsson, M. G., Shao, L., Carlton, P. M., Wang, C. R., Golubovskaya, I. N., Cande, W. Z., ... & Sedat, J. W. (2008). Three-dimensional resolution doubling in wide-field fluorescence microscopy by structured illumination. *Biophysical journal*, 94(12), 4957-4970.
- [10] Zhang, Han, Ming Zhao, and Leilei Peng. "Nonlinear structured illumination microscopy by surface plasmon enhanced stimulated emission depletion." *Optics express* 19, no. 24 (2011): 24783-24794.

- [11] Manish Saxena, Gangadhar Eluru, and Sai Siva Gorthi. Structured illumination microscopy. *Advances in Optics and Photonics*, 7(2):241, June 2015.
- [12] Gustafsson, M. G. (2005). Nonlinear structured-illumination microscopy: wide-field fluorescence imaging with theoretically unlimited resolution. *Proceedings of the National Academy of Sciences*, 102(37), 13081-13086.
- [13] Xu, D., Ding, J., & Peng, L. (2020). Structured illumination imaging with quasi-periodic patterns. *Journal of biophotonics*, 13(6), e201960209.